

The Flight Instrument Design for the Terrestrial Planet Finder Interferometer

Stefan Martin

Jet Propulsion Laboratory, California Institute of Technology, Pasadena, California 91109

ABSTRACT

The direct optical detection of Earth-like planets orbiting nearby stars is the goal of the Terrestrial Planet Finder Interferometer (TPF-I). At infrared wavelengths between about 7 and 17 μm , spectral absorption features in the thermal emission of such planets may indicate the presence of chemical compounds thought necessary for the existence of life. To perform nulling interferometry at these relatively long wavelengths, a long baseline telescope array is needed with an overall length between about 30 m and 200 m. The current flight design effort is concentrated on the dual chopped Bracewell architecture but the design of the flight instrument is to a large degree independent of the exact array layout. Four 4 m diameter telescopes employing a conventional three-mirror design collect the light from the star and a series of sensors and actuators direct the light to a separate beamcombiner spacecraft where a number of beam control actions take place prior to the science light detection. This paper describes the opto-mechanical systems of the telescopes and beamcombiner spacecraft including the wavefront and optical path control devices and the alignment systems. The mechanical layouts of the spacecraft are described along with the predicted performance of the structure in terms of thermal and vibration control. The layout of the control system is also described.

1. INTRODUCTION

The Terrestrial Planet Finder Interferometer (TPF-I) is a mid-infrared formation-flying space interferometer. Together with its sister mission, a visible-light coronagraph (TPF-C), it will characterize Earth-like planets orbiting nearby stars. TPF-I will use nulling interferometry techniques to reduce the glare from the parent star and enable the analysis of the planet light by spectroscopic observations. To spectroscopically characterize planets with sizes down to half the apparent area of the Earth requires a large telescope collecting area and stable performance for long integrations of light from the system being observed. TPF-I operates at wavelengths between 7 and 17 microns. At these wavelengths, not only are planet spectral features expected to be scientifically interesting, but also the contrast of near one million to one between the star and planet is favorable for planet detection; at optical wavelengths it is for comparison as much as 10^{10} . At these longer wavelengths, the observatory size needs to be large to achieve sufficient angular resolution to separate the planet from the star. Using the technique of interferometry an effectively large telescope can be built by combining the light from a few smaller individual telescopes separated in space. To achieve the desired resolution the telescopes will be separated by between 30 m and more than 100 m.

To observe an exoplanetary system using the dual Bracewell layout, the array must be assembled in line with the beamcombiner spacecraft off-axis near the center (see artist's concept Figure 1). The telescope separations will depend primarily on the angle subtended by the habitable zone as seen from Earth. Normally the light from the telescopes will be combined by nulling the light from telescope 1 (T1) and T3 and combining the output with the nulled light from T2 and T4, but a T1-T2 and T3-T4 combination would also be used for certain planetary systems. An initial observation to determine if there are objects of interest around a star would take about 10 hours, depending on many factors, during which time the array would rotate a full 360° around the line of sight. Stars outside a band greater than 45° away from the ecliptic would not be observable since the solar shades will no longer protect the telescope assemblies from heating by the sun.

The two types of spacecraft which form the array are: inner and outer collector spacecraft, and a single combiner spacecraft. The collector spacecraft collect the light from the target system and relay it to the combiner spacecraft via a second collector spacecraft. The additional transfer is required by the dual Bracewell configuration in order to equalize the optical path lengths- in the X-array concept (telescopes arrayed at four corners of a rectangle with the combiner central), each beam would instead be transmitted directly to the beamcombiner spacecraft. The beam paths from the inner spacecraft differ from those for the outer spacecraft, so there are detail differences between the outer and inner spacecraft, but in this work we have designed collector spacecraft which are interchangeable should a unit be lost from the array. The



Figure 1: TPF-I Flight formation of telescopes.

formation flying. The spacecraft also have RF systems for communications both between themselves and the ground and RF sensors for coarse formation flight control.

The spacecraft carry enough propellant to allow the complex maneuvering that the observations require for a mission duration of a minimum of five years. While some mission configurations have employed a single launch, for this study we allowed launching in two heavy vehicles, giving sufficient mass and size margin to allow larger telescopes to be carried. When the collector spacecraft are released from the cruise vehicle, two major deployments will take place; the deployment of the sunshade and the deployment of the telescope secondary mirror, beam transfer optics and cylindrical shade. These latter systems are folded down for launch to reduce the volume of the system. The principal deployment of the combiner spacecraft is the sunshade.

The work described in this paper covers a first look at the flight instrument design for the Formation Flying Interferometer, including the optical system and beam train, the control system and sensors, and the thermal and dynamic environments. This work followed on from earlier work by the team on a structurally connected interferometer (SCI) version. The SCI design employs many of the systems used in the FFI design, but was more limited in the number of stars it could observe. For this FFI design study, we used some systems from the SCI design and modified others in order to look at some different approaches. For example, most of the control system was reworked to accommodate the separate spacecraft and the modified Mach-Zehnder (MMZ) nuller design was replaced by a simplified nuller. Collector telescopes were also redesigned to improve their performance during observing mode. Much work remains to be done, including trade studies in metrology and alignment systems and in path length control, and greater detail needs to be added in all areas. The following presents a snapshot of the design at the conclusion of our initial design effort earlier this year.

2. OPTICAL BEAM TRAIN

2.1. The collector spacecraft

The beam train consists of the following main elements. First the collector telescopes, a three-mirror design. Beneath the telescope primary mirror, see figure 2, are systems for maintaining pointing at the star and internal alignment and metrology systems. A deformable mirror (DM) is included in the beamtrain to allow wavefront correction; further analysis will be needed to examine the necessity for this unit and its range of operation. Following recollimation of the beam, a number of fold mirrors transmit the beam up to near the top of the telescope body and send it to the next spacecraft. The next spacecraft then relays the beam to the beamcombiner spacecraft.

combiner spacecraft receives the optical beams from the collectors and combines them to produce the signal, and therefore has a very different architecture.

The spacecraft are equipped with a five-layer square shaped sunshade that permits the bulk of the optical system to be maintained at about 40K by passive cooling. Some parts of the system on the beamcombiner are actively cooled to lower temperatures, notably the science detector at 7K. These low temperatures minimize the self-radiation of the optical beam train which would add a noise signal to the science light. Spacecraft electronics and mechanical components are placed on the side of the spacecraft exposed to the sun and are maintained near room temperature. Additional components include reaction wheels and small thrusters for

2.2. The combiner spacecraft

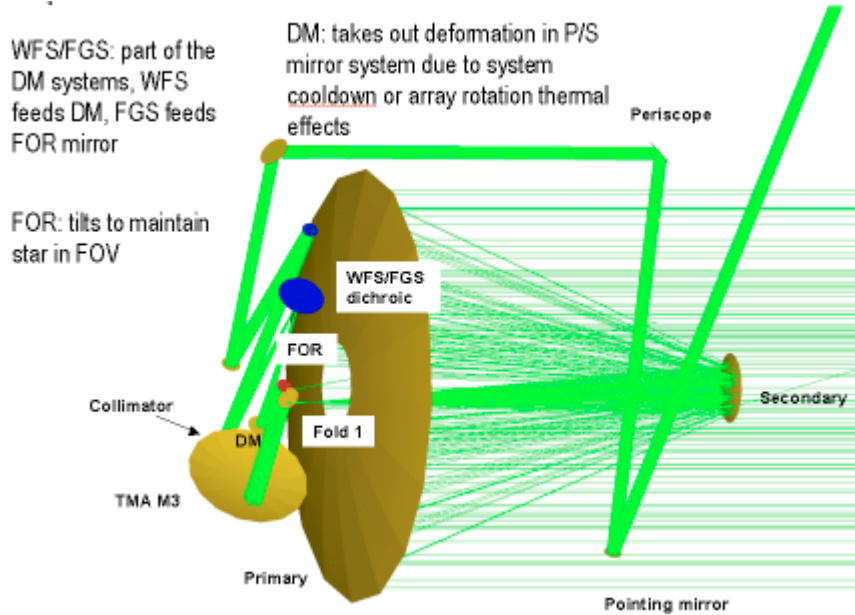


Figure 2: The main optical components of the collector telescope spacecraft.

On the beamcombiner spacecraft, the beam is first compressed from approximately 150 mm diameter to 30 mm diameter and passes through a multistage delay line. Following the delay line it enters the adaptive nuller where the phase and amplitude are adjusted across the spectral band. After the adaptive nuller it enters a switch which allows selection of T1-T2, T3-T4 or T1-T3, T2-T4 beam combination and then it enters the nuller itself at which point the fringe tracking light is separated from the science beams. After nulling and interfering the beams at the appropriate phases the science light enters a single spatial mode fiber and then is dispersed spectrally before striking the science detector. Numerous beam train systems exist to maintain and adjust alignment and phase of the beams; these will be discussed below.

2.3. Telescope assembly

The telescope design is a three mirror anastigmat design using conic sections: the primary is an ellipse, the secondary is an hyperbola and the tertiary is an ellipse. After reflection from the secondary, the beam passes through a hole in the center of the primary and is folded by a plane mirror into a plane beneath the primary. The primary mirror has a diameter of 4.0 m, and the secondary a diameter of 0.3 m giving an obscuration ratio of ~ 0.023 (excluding spiders and mounts). An offset field angle used in previous designs was eliminated to reduce the number of differences between the left and right sets of collector telescopes. The new design was also required to have a very uniform wavefront performance across the field of view. This is to ensure that as the telescope drifts in space, the Strehl ratio remains the same, so that the coupling onto the single mode fiber at the end of the beamtrain does not vary. This ensures that the null depth will remain constant during the observation. It was not considered desirable to continuously operate the DM to compensate for these small wavefront changes. A mirror under the telescope base acts as a field of regard (FOR) mirror; it tilts to bring light from a chosen star into the main beam path and maintains that alignment continuously during observations.

The main design requirements are:

Field of view:	1 arc min radius
Primary aperture:	4000 mm
Wavefront quality:	≤ 200 nm rms wavefront error including uncompensated manufacturing and alignment tolerances. Nominal design residuals are ≤ 60 nm rms wavefront error.
Uniformity:	Strehl ratio variation $\leq 2 \cdot 10^{-4}$ over FOV
Exit pupil:	Corresponds to 22 nm rms wfe; current allocation for design is $0.5 \cdot 22 = 11$ nm Real, maximum diameter ≤ 150 mm to accommodate cryo DM

2.4. Beam train optics

Beneath the primary mirror the beam strikes a fold mirror which tilts to bring the starlight into the main beam path. Next it strikes the third mirror of the three-mirror telescope and the field of regard dichroic mirror. Behind this dichroic mirror are an alignment beam launcher and a metrology beam retroreflector. Next, the beam strikes the DM, which corrects static wavefront errors. This pair of mirrors (the DM and the FOR) is controlled from the output of sensors placed

behind the WFS/FGS dichroic, next in line, which separates out some light from the star for pointing and wavefront sensing. Next the beam is recollimated and transmitted to the top of the spacecraft. An active pointing mirror relays it to the next spacecraft.

2.5. Beam transfer between spacecraft

The active pointing mirror is controlled by beam shear sensors located behind a mirror on the next spacecraft. This continuously relays signals via an RF system to maintain accurate pointing. For interspacecraft transfers, the mirrors are arranged so that there is maximum shielding of the mirror from the sunshade of the next spacecraft. This is important for stray light mitigation. In earlier TPF-I designs, the number of folds and their angles were maintained in a symmetric

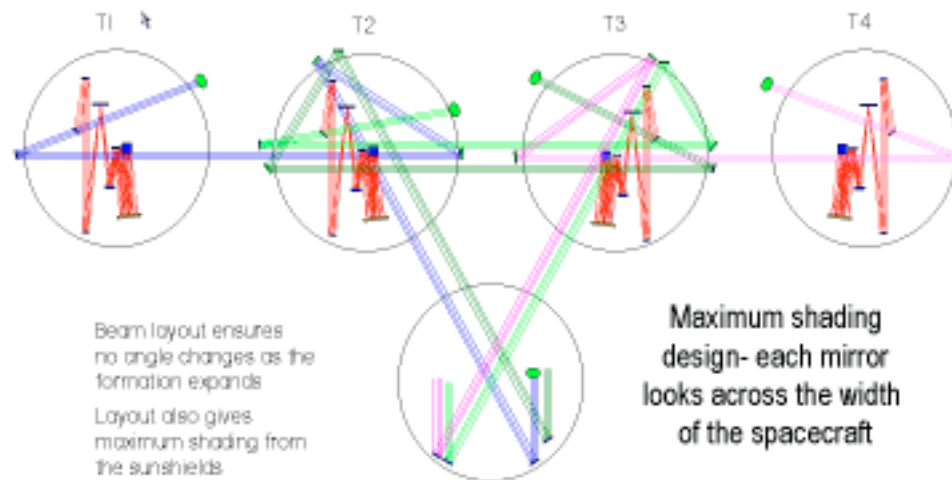


Figure 3: Beam transits between spacecraft are made as nearly as possible across diameters.

extremely low levels of light from the target. Two stray light analyses were performed, one a simple spreadsheet analysis and the other using an optical model known as FRED. Good agreement was obtained between these models for collector-collector transfers. Both models showed that for beam transfer heights 4 m above the sunshades, the collector-collector separation could be as much as 165 m. Baffle diameter was 125 mm at the transmitting spacecraft and 150 mm and the receiving spacecraft. Further analysis is needed for beam transfers between collector and combiner.

2.6. The combiner spacecraft

The combiner spacecraft contains the majority of the optical systems. Each beam train is replicated exactly with minor differences at the simplified nuller. The top of the spacecraft receives the beams in a maximum shading arrangement and folds them down onto one side of a two-sided vertical main bench, see Figure 4. Here the beams are compressed to 30 mm diameter and passed through multistage delay lines before passing through to the opposite side of the bench and entering the adaptive nullers as shown in Figure 5. At the output of the nullers the beams are sent to the switch and into the nuller. The exit pupil of the adaptive nuller forms the pupil of the beamcombiner system. The nuller bench is appended to the base of the vertical bench.

2.7. Beam conditioning

The beam conditioning systems are: pupil stops and apertures to define the beams and restrict stray light, DM (on the collector spacecraft), adaptive nuller to tune amplitude and phase across the spectrum, delay lines for coarse through fine stages of fringe acquisition, and pointing and shear detectors for both interspacecraft beam transfers and for internal alignment principally on the beamcombiner spacecraft. Another system needed in the FFI design allows adjustment of the polarization angle of the incoming beams which can change as the spacecraft drift. The final system is the single mode

fashion for each beamtrain. In this design, the fold angles are allowed to vary to allow easier engineering of the layout and the resulting small asymmetries are compensated for by the adaptive nuller.

2.5.1. Stray light modeling

Analysis showed that for a beam transfer mirror a view of the opposite spacecraft's sunshade, particularly the gap between the topmost shades, would admit an excessive number of stray light photons into the science beam. This is because of the small imperfections of real mirrors and the need to detect

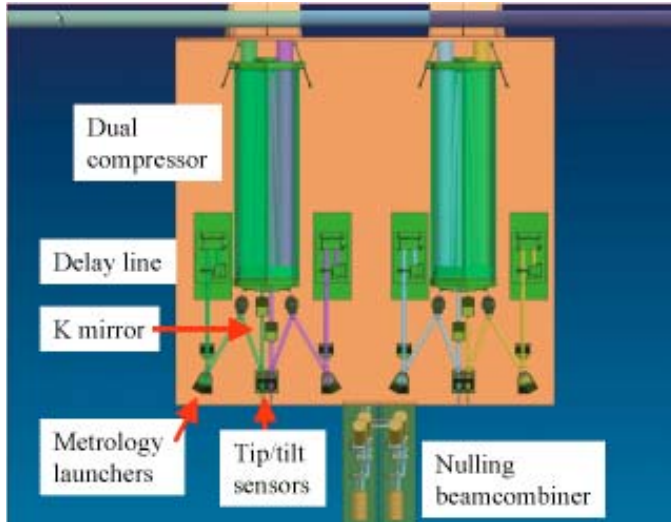


Figure 4: First side of the vertical optical bench.

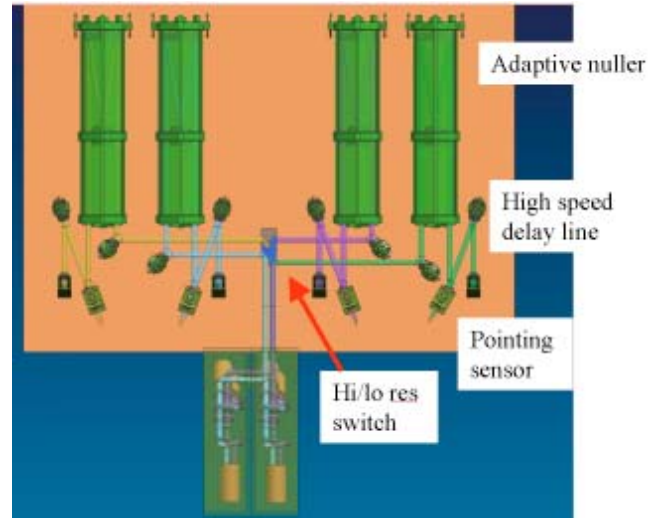


Figure 5: Second side of the vertical optical bench

spatial filter placed before the science detector, this selects the fundamental mode of the beam and reduces the sensitivity to shear and pointing misalignments as well as higher order beam asymmetries.

2.7.1. The adaptive nuller

The adaptive nuller² consists of a deformable mirror placed at the focus of a parabolic mirror in an arrangement similar to a cat's eye delay line. At the focus, the input beam is dispersed in wavelength and separated into two orthogonally polarized stripes. By pistoning the mirror elements, phase can be added or subtracted from different spectral regions of the beam and by tilting the mirror elements across the length of the stripe the pointing of the output beam can be varied. By

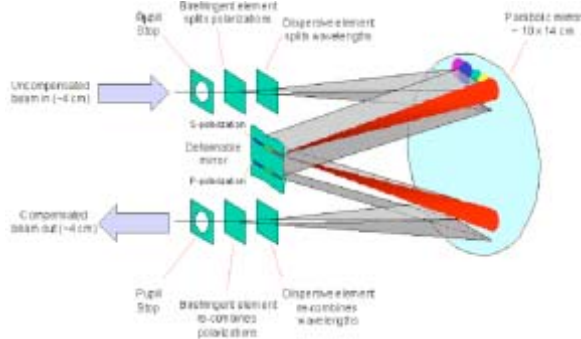


Figure 6: The adaptive nuller.

clipping the output beam against an aperture, the beam intensity can be varied for a particular range of wavelengths. One of these systems is placed in each beam and allows the correction of small differences in throughput and phase between beams arising from alignment changes and variations between optical components throughout the beam train. This capability operates independently on both polarizations.

2.7.2. The delay lines

A multistage delay line is conceived for this system. A coarse stage of >20 cm range allows initial acquisition of the fringe and it is then parked. Subsequent stages allow range adjustment from 50 pm to 5 cm in three stages. The fine stage is a high speed stage based on a similar concept to stages

used in JPL's Planet Detection Testbed³. These are reactuated piezoelectrically driven stages capable of moving a 50 mm diameter mirror a distance of 3 μm at a rate of more than 2 kHz. The fine stage is a separate item mounted on the second side of the optical bench. The other two stages form a single unit with voice coil actuation. The operating ranges of the three stages overlap the regions 50 pm to 50 nm, 50 nm to 50 μm and 50 μm to 50 mm.

2.7.3. The alignment system

Pointing and shear detectors are located at various stages in the system. A full-aperture alignment beam produced by a laser mounted on the collector spacecraft is coaligned with the science light and used for beam shear or pointing sensing

at interspacecraft transfers, after the compressors and after the adaptive nullers. The same beam is used for polarization angle sensing and correction on the beamcombiner spacecraft immediately after the compressors. Pointing adjustments are made at the last mirror transmitting to the next spacecraft, at the entrance to the compressor and possibly at the entrance to the nullers (depending on the predicted stability). Pointing and shear corrections are made at the entrance to the adaptive nuller.

2.8. The simplified nuller

For the FFI design work, one desire was to try to simplify the MMZ nuller used on the SCI design. The main benefits would be that only one internal laser metrology beam would be needed for each beam of the interferometer rather than two, the attenuation or round trip insertion loss would be less for the metrology light, and the science light would emerge on only two beams rather than four, offering a small but significant improvement in signal to noise ratio at the detector. There would also be associated engineering simplifications. Because of the wide spectral band to be covered by TPF-I, the nuller is actually divided into two units stacked next to one another, one operating on the wavelength range 7 to 11 μm and the other on the range 11 to 17 μm . This arrangement necessitates an additional metrology path and possibly a second fringe tracking system. By splitting the spectrum we generate less demanding coating requirements on

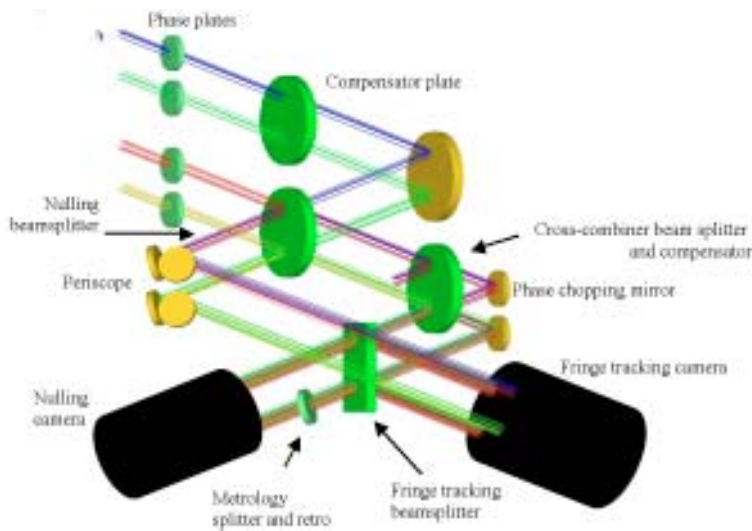


Figure 7: The simplified nuller.

focused through the single-mode spatial filter (subject of a TPF-I technology development effort) and then dispersed through a prism before sensing on the science array. Since only two beams are output from each cross-combiner, the science detector design (nominally a Si:As array) handles all four beams from the pair of cross-combiners.

The nuller layout includes a fringe tracking camera which detects the phase on each nuller and on the cross-combiner. One beam from each nuller is extracted from the rejected light output (all the 7 - 17 μm wavelength starlight exits the system from this output) and is dispersed onto the camera array. From the cross-combiner, two beams are extracted, so a total of four beams is sensed at the array. For the second cross-combiner a second fringe tracker would be needed unless a laser metrology could be used to transfer measured phase to the second nuller.

3. CONTROL SYSTEM

With so many moving parts the observatory requires an extensive control system. The basic requirements for nulling performance to meet our planet detection goals imply amplitude control of the incoming beams to 0.1%, and phase control of the beams to 2 nm across the band. In turn the amplitude control requirement can be broken down into a pointing and shear requirement at the input to the spatial filter. Mirrors that move cause translation of the beams at other mirrors and

the beamsplitters which must give a near 50/50 split for the highest efficiency. Also, single spatial mode filters which cover these spectral bands are expected to become available.

The simplified nuller uses a beamsplitter/compensator plate arrangement to obtain a near-match of optical path across the waveband. Residual error in reflection/transmission ratio (R/T) is taken up using one specially fabricated coating on one side of the compensator plate. Models showed that throughput could then be matched across the spectral band on both incoming beams to better than 1%. The residual amplitude and phase errors are then well within the compensation range of the adaptive nuller.

2.9. Science detector and fringe tracking

The science detector operates on the two complementary outputs of the cross-combiner. Light emerging from the cross-combiner is

because of mirror imperfections and non-uniformities this can change the phase and distribution of phase and amplitude across the passband, changing the null depth and introducing a noise component into the signal. The full complexity of these and other effects, for example diffraction effects over long beam paths, is yet to be modeled but the basic layout of the control system can be deduced from experience in the nulling laboratory and the modeling that has been done so far. In smaller systems null depths of 10^{-6} , adequate for the performance needs of TPF-I, have been reached using monochromatic light⁴ and work is in progress to extend these results to broader spectral bands⁵ and to systems which null on two pairs of beams. The Keck Observatory's nuller^{6,7} control system also shares features of the TPF-I design although the layout is somewhat different. The Planet Detection Testbed incorporates a number of the control systems envisioned for TPF-I.

For deep nulling, the optical properties of the two incoming beams need to be matched to a high degree⁸. The single mode spatial filter can alleviate some of these requirements, so for example, incoming beam tilt and shear errors do not have to be so finely controlled as a simple analysis would suggest. Even so, for the flight design the pointing requirement will be of order 1 arc sec, and the shear requirement about 1.2% of beam diameter. The polarization rotation angle matching requirement is about 2 arc minutes. The telescopes can drift in space to angles up to 1 arc min from the star and this would result in a similar rotation of the polarization of the telescope's output beam. After transfer through the second collector and into the beamcombiner, and allowing for static errors in the setup, the requirement could be exceeded unless correction is possible.

The basic control scheme is laid out in the series of figures 8 through 11. Some alignments will take place continuously and others will take place occasionally; these have been differentiated using different colors for calibration phase and

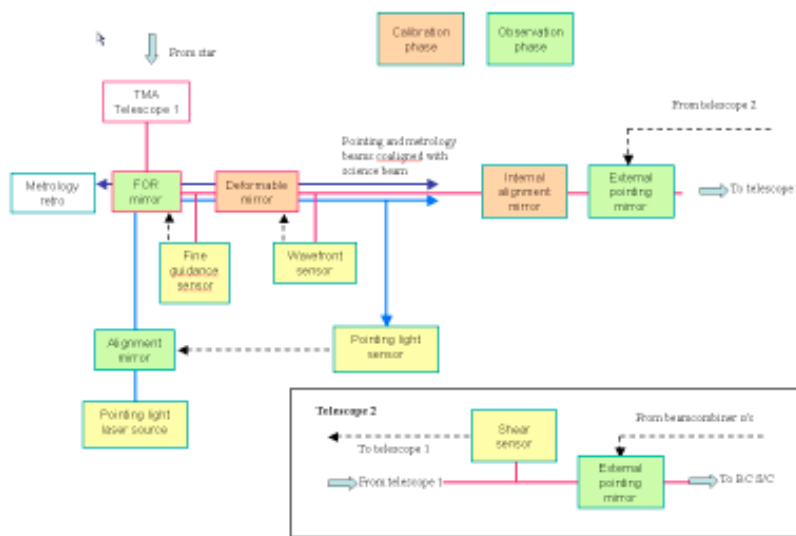


Figure 8: Control scheme: telescope spacecraft.

sensor allows correction of any primary mirror aberrations. A metrology retroreflector reflects full-aperture metrology, coaligned with the starlight, back to the beamcombiner spacecraft. An internal alignment mirror is included to facilitate any necessary post-launch adjustments, and then the science beam and alignment beam leave the telescope spacecraft via a pointing mirror. This pointing mirror is controlled from a shear sensor located on the next collector spacecraft, requiring a slow control loop running through the RF link. Similarly, a pointing mirror on the second telescope is controlled by a shear sensor on the beamcombiner spacecraft (lower box on figure 8). Thus, the science light, alignment and metrology beams arrive at the beamcombiner spacecraft.

Figure 9 shows the first section of the beamcombiner beamtrain. A coarse pointing mirror controlled from a sensor further down the beamtrain directs the light through the compressors and K mirrors. The K-mirrors are controlled by tilt sensors located next in line, allowing small angular deviations in the polarization vector of the science beam to be controlled. Next the beams pass the metrology injection point (figure 10) where two sets of laser metrology are directed up to the telescope retro and also down to the beamcombiner retro at the end of the beamtrain following the cross-combiner. The beams enter the delay lines which are controlled by inputs from the downstream fringe trackers and also from the laser

observation phase processes. Calibration-phase processes might take place once every few hours up to once every few days, depending on the stability of the systems involved. Observation-phase processes will have characteristic times of milliseconds up to minutes.

3.1 System summary

The system is briefly summarized here and more detail is added in the following section. Referring to figure 8, starlight enters the main beam train at the FOR mirror and propagates to the beamcombiner. A fine guidance sensor behind the dichroic mirror controls the FOR mirror and maintains pointing on the star. A pointing light sensor and an alignment mirror allow the starlight and an alignment beam to be accurately coaligned in the beamtrain. Also, a wavefront

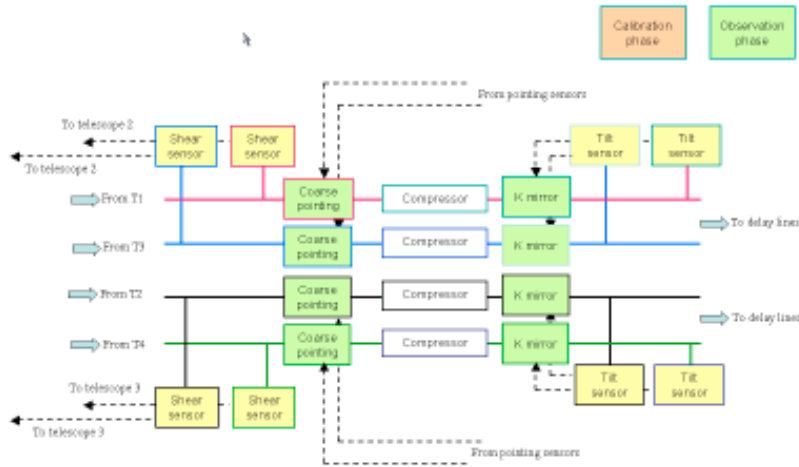


Figure 9: First section of beamcombiner spacecraft control system.

metrology gauges. The high speed delay line is in fact located separately slightly further down the beamtrain. The beams are then accurately aligned in shear and pointing prior to entering the adaptive nullers. Accurate prealignment is necessary here because the adaptive nullers rely on controlling beam shear and pointing at the output, so these parameters must be fixed at the input. Therefore, the pointing and shear sensors immediately precede the adaptive nullers; these same sensors also control the coarse pointing mirrors previously mentioned. Each laser metrology beam has its own alignment mirror which would only be adjusted occasionally.

The adaptive nuller control is set up during the calibration phase using data acquired by the science camera, removing

small amplitude and phase differences across the waveband so that the nulling performance can be optimized.

Figure 11 shows the final section of the beamtrain. Only one set of nullers is shown but there would also be a split to separate the 7 to 11 μm waveband from the 11 to 17 μm waveband. After the split, a second set of pointing sensors is required to actuate fast pointing mirrors which control the final part of the beamtrain. The beams then enter the nullers, and at the exit an optical path chop is applied in one beam, controlled by the OPD control system utilizing both fringe tracker and metrology data. The science beams are then cross-combined and the internal laser metrology is retroreflected to the launchers. Finally the science beam is filtered to a single spatial mode, dispersed and focused onto the science camera.

3.2. Optical alignment

A polarized laser beam is launched from behind the FOR mirror on each collector towards the combiner. See figure 12. This beam is used throughout the beamtrain for the pointing and shear metrology and for polarization rotation metrology.

3.2.1. Pointing metrology

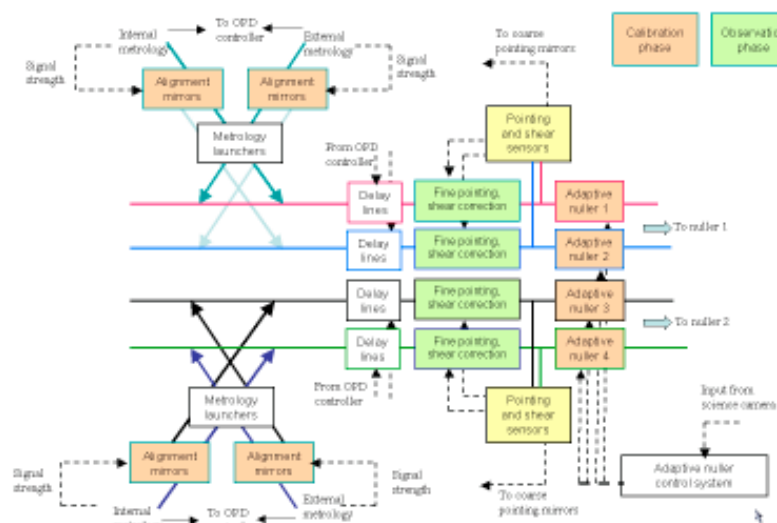


Figure 10: Second section of beamcombiner spacecraft control system.

Short wavelength radiation from the star (0.8 to 1.0 μm) is focused onto a sensor behind the dichroic mirror on the collector spacecraft. Its position on the sensor is controlled by the FOR mirror, thus forming a loop controlling the angle of the starlight with respect to the beam train. A polarized laser beam of wavelength 850 nm is launched behind the FOR mirror and sensed on another sensor behind the dichroic mirror also shown in figure 12. The laser beam is pointed using a tilt mirror behind the FOR mirror, thus forming another closed pointing loop. Calibrations can be made to coalign the stellar beam and the laser beam by integrating the starlight on the laser sensor with the laser turned off. Thus, a bright reference beam for the science beam is formed and can be used downstream for maintaining alignment.

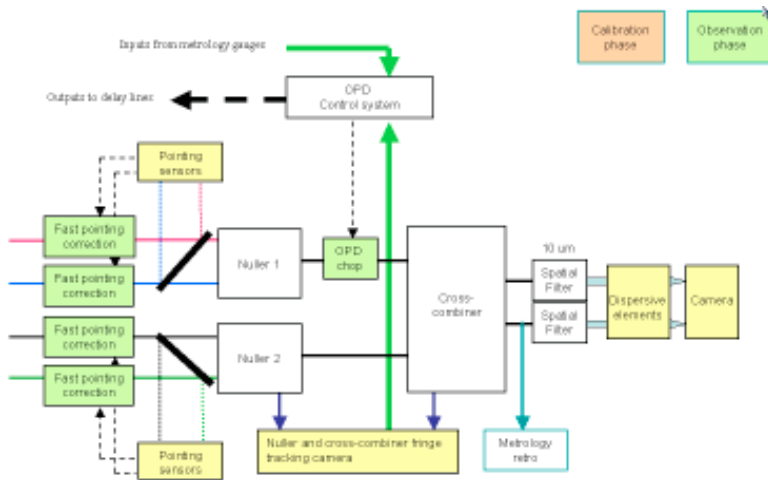


Figure 11: Final section of beamcombiner spacecraft control system.

Shear is first sensed after transfer to the next collector by a dichroic mirror with a set of lenses placed behind it (figure 13). This dichroic lets through a portion of the 850 nm radiation but reflects most of it together with all the other useful light. The sensor output is run back to the transfer mirror on the first spacecraft to point the beam at the center of the dichroic shear sensor mirror. An identical method is used for transfer to the beamcombiner spacecraft. Once inside the beamcombiner the shear is again sensed after the delay lines and corrected before entry to the adaptive nullers.

3.2.3. Polarization rotation

Polarization rotation metrology uses the same laser beam as the pointing system; the beam is initially polarized and this forms a reference for beamtrain induced rotations of the polarization angle. On arrival at the beamcombiner spacecraft the beam is compressed and then passed through a K-mirror assembly which allows the polarization angle to be rotated. A polarization angle sensor is placed immediately after the K-mirror, thus a loop can be formed to allow continuous correction of the polarization angle.

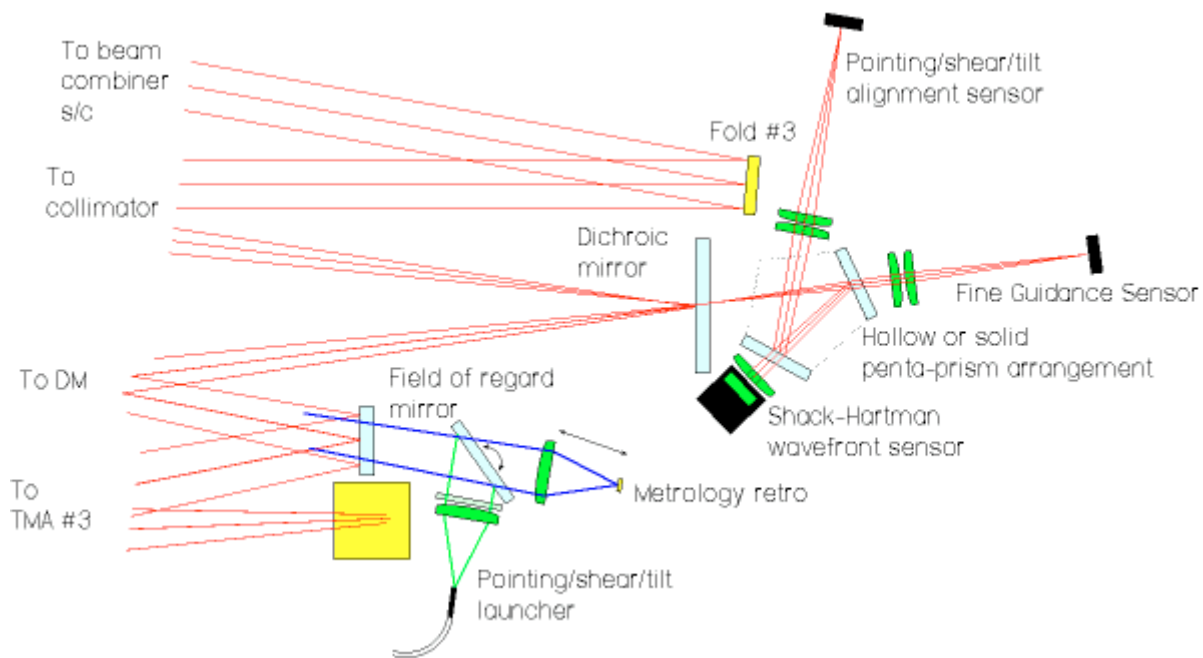


Figure 12: Telescope ancillary optical components.

The beam angle is also sensed and corrected on the beamcombiner spacecraft just before entering the adaptive nullers. Simple lens and quad cell assemblies suffice for sensing and a high speed tip/tilt mirror corrects the angle in conjunction with a coarse pointing mirror located at the input to the compressors. An additional stage of pointing correction is needed before entry to the beamcombiner to allow for misalignments introduced by the switch and 11-17 μm split.

3.2.2. Shear metrology

Shear metrology uses the same laser beam as the pointing system; the two systems are closely coupled. By placing a pupil stop at the FOR mirror, the alignment laser beam and the starlight have the same initial shear.

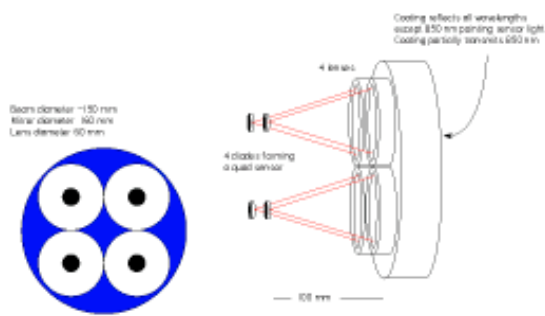


Figure 13: Transfer mirror shear sensor.

the star and typically will sense some 10^7 photons per second. Calculations show that the response time of the fringe tracker will be ~ 0.01 second and the OPD control time constant will therefore be ~ 0.1 second. This is most likely inadequate given that the expected spacecraft vibration will extend to many tens of Hz with appreciable amplitudes (see below). Therefore a laser metrology system operating at wavelengths near 1550 nm is used to sense and allow control of the higher frequency vibrations using principally the high speed stage of the delay line.

This polarization control loop is needed because although the adaptive nuller can in principle correct for the rotation error by adjusting intensities, it cannot do so on the timescales consistent with formation drift motions. Note that there is an unsensed rotational component caused by clocking of the telescopes around the line of sight to the star; this would need to be known and sensed by means probably involving transfer mirror angle knowledge.

3.2.4. OPD metrology

The OPD metrology system forms part of the fringe tracking system and effectively extends the frequency response of that system up to several hundred Hertz. The fringe tracker relies on light from

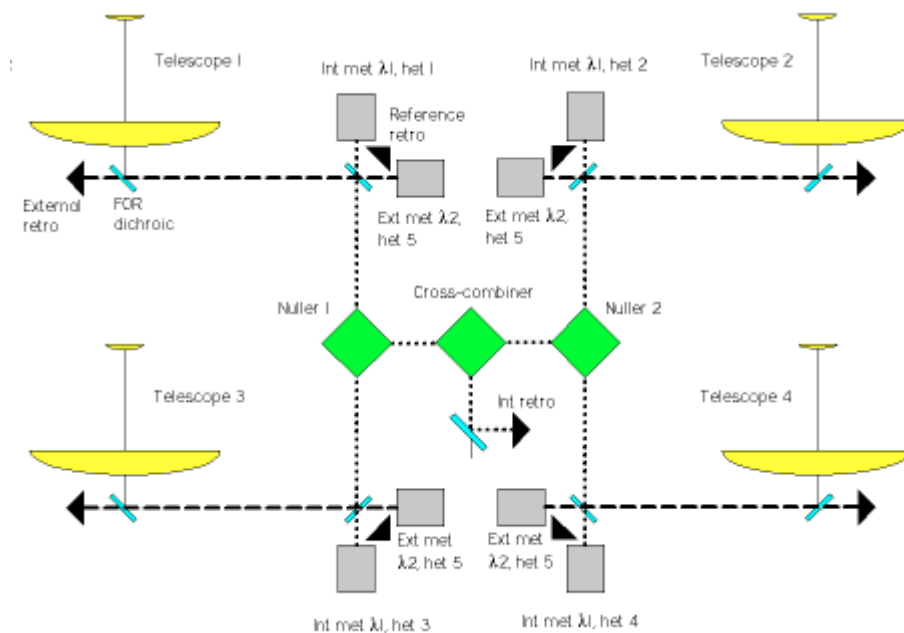


Figure 14: Metrology scheme for simplified nulling beam combiner.

heterodyne frequencies. External metrology extends from the same launch dichroic to a retroreflector placed behind the FOR mirror. These beams could all run at the same frequency shift, assuming no interference via the beamcombiner retroreflector, but would have a different wavelength from the internal metrology, nominally 1570 nm. The reference point for both internal and external metrology is at the launch dichroic, a complex custom optic. Metrology pointing is active during calibration periods and consists of adjusting the mirrors placed behind the launch dichroic to maximize the return signal from the collector and combiner retroreflectors. Once set, these should require infrequent adjustment since the alignment is maintained by the separate alignment system.

Key elements of the metrology system are: it fills the aperture of the science beam, it measures down to the last beamsplitter, and it measures as far as possible only internal optical path. One area of the beam train is unsensed at present, that is the section from the FOR mirror to the primary mirror. It is worth noting that one possible motion cannot in any case be sensed and that is high speed motion of the primary mirror with respect to the star; more on this issue later. The metrology system is divided into two components, internal and external, as shown in figure 14. Internal metrology extends from the launchers just ahead of the delay lines down to a single retroreflector following a dichroic mirror placed after the cross-combiner beamsplitter. Beams from the four input paths are differentiated by having different

nullers, the high/low resolution switch, and the shear and pointing sensors and actuators. The whole assembly will be contained within a cylindrical cover. The adaptive nullers (see figure 18, a side view) are angled away from the bench because they have prisms at the entrance and exit which refract the light away from the plane of the bench.

The nullers are built as a separate unit attached to the base of the bench (figures 16 and 18) together with the fringe tracking cameras and the science detector. These detectors could alternatively be attached to the vertical bench and the light would be brought in via optical fibers. Below the vertical bench (not shown) is a thermal shield separating it from the spacecraft main bus and the other spacecraft systems including the solar shade. Since the science detector requires cooling to 7K, the bus also carries a cryocooler.

5. THERMAL MODELING

A limited amount of thermal modeling has been done on this design. A model originally developed by Ball Aerospace was used to test the thermal environment with the spacecraft in close proximity and in a separated formation. Also, the X-array configuration was briefly looked at. Results showed that the sunshades of the collector telescope spacecraft produce passive cooling down to 24 K at the secondary mirror, with little difference between close and widely separated configurations. These temperatures meet our targets for the beamtrain optics, but the primary mirror (40 K) was at the target temperature, meaning that there is no margin here. The results exclude the influence of any cold side heat sources which will need to be maintained at low power, so that the relatively high primary mirror temperature is a cause for concern. Some changes could be made to improve this for example, increasing the inter-shade angle (currently 0.5°) and spacing (currently 75 mm) per shade would reduce the primary mirror temperature. Colder sections of the optics (a small part of the beamcombiner and the science detector) will be actively cooled by the cryocooler which needs to be added to the model. Additional work needs to be done to provide a thermal model of the instrument payload both on the collectors and combiner, including the optical benches with their optics, actuators and sensors.

6. STRUCTURAL MODELING

Some structural modeling was done on the collector telescopes to look at the effect of vibration from the reaction wheels on two of the main mirrors and at the effect of thruster firings. This modeling effort is detailed in another presentation to

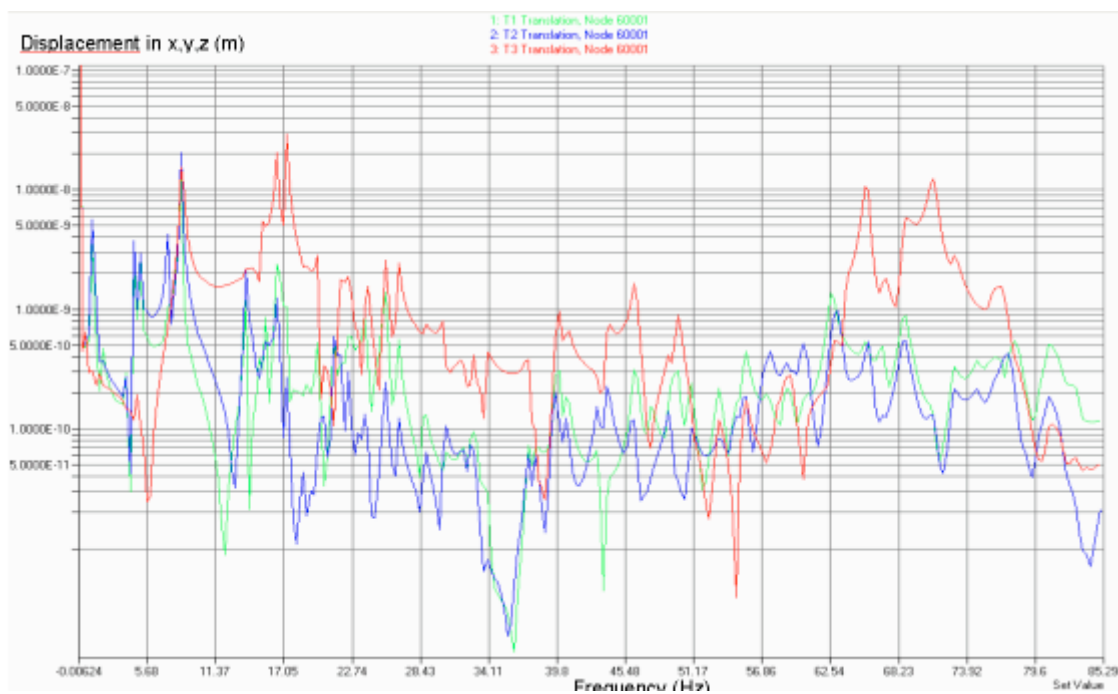


Figure 18: Induced motion of secondary mirror caused by reaction wheel vibration.

this meeting⁹ and so will not be repeated here. From an instrument perspective the main findings are that the motion of the secondary mirror along the optical axis may exceed 1 nm over much of the spectrum, as shown by the uppermost trace in figure 18. Below 28 Hz, the amplitude varies but peaks at more than 10 nm near 17 Hz. Also between 60 and 80 Hz, amplitudes are large. They exceed the rate which can be corrected by the fringe tracker and they are in the section of the beam train which is not monitored by laser metrology which stops near the FOR mirror. However, on the positive side, the vibration amplitudes are sufficiently small that it is possible that vibration mitigation efforts would reduce them sufficiently. Such mitigations might be: improved isolation of reaction wheels, or no reaction wheels and spacecraft controlled by proportional thrusters or another low vibration system. Lacking an error budget for the beamtrain, it is difficult to say what the vibration level should be, but it is likely to be significantly less than 1 nm for frequencies greater than a few Hz. In the worst case, a laser metrology system could be added to the telescopes to measure much of the unmonitored path. Primary mirror vibrations were typically an order of magnitude smaller, so they are much less likely to cause concern. Additional work to look at the major bending modes of the primary is also desirable.

7. CONCLUSION AND SUMMARY

Basic optomechanical and thermal designs have been produced for both the FFI and SCI systems. The optical models include the whole beamtrain from the telescopes through to the beamcombiner.

Controls systems have been identified and incorporated into the layout and high speed control links isolated onto individual spacecraft with only relatively low bandwidth links being needed between spacecraft.

Thermal modeling of the array confirmed earlier work performed at Ball Aerospace and radiation effects between adjacent spacecraft appeared to have a minimal thermal effect. The initial thermal situation looks promising with collector temperatures at ~30K and combiner temperatures at ~40K, with heat sources needing to be added.

Stray light passing from the sunshields to the transfer mirrors limits the interspacecraft spacing to 165 m; to achieve this result we placed the transfer mirrors high on the spacecraft near the telescope secondary mirrors.

Structural models show that the vibration environment on the telescopes needs to be improved because vibrations produced by the reaction wheels are of a sufficient amplitude that they could limit the mean null depth.

Overall the TPF-I Flight Instrument Team has illustrated a viable design outline for the space interferometer and no insurmountable difficulties have been encountered.

ACKNOWLEDGMENTS

There have been many contributors to this work. Amongst them I would particularly like to thank Ron Holm, Jose Rodriguez, John Cardone, Hong Tang, Ying-Yong Li, Zahidul Rahman, and Douglas Adams at the Jet Propulsion Laboratory, John Galloway, Mark Wilson, June Tveekrem, Claef Hakun at Goddard Space Flight Center, and Charley Noecker at Ball Aerospace.

The work reported here was conducted at Jet Propulsion Laboratory, California Institute of Technology, under contract with NASA. Reference herein to any specific commercial product, process, or service by trade name, trademark, manufacturer, or otherwise, does not constitute or imply its endorsement by the United States Government or the Jet Propulsion Laboratory, California Institute of Technology.

REFERENCES

1. "TPF- A NASA Origins Program to Search for Habitable Planets". Edited by C.A. Beichman, N.J. Woolf, and C.A. Lindensmith. Jet Propulsion Laboratory, Pasadena, CA. JPL Pub 99-3 5/99 (1999).
2. "Near-IR demonstration of adaptive nuller based on deformable mirror". Peters, Robert D.; Hirai, Akiko; Jeganathan, Muthu; Lay, Oliver P. Proceedings of SPIE Volume: 5491. "New Frontiers in Stellar Interferometry". Editor(s): Traub, Wesley A. Published: 10/2004
3. "TPF Planet Detection Testbed: demonstrating deep, stable nulling and planet detection". Stefan Martin. IEEE Aerospace Conf. Proceedings, Big Sky, Mt, 2005.

4. "Mid-infrared nuller for Terrestrial Planet Finder: design, progress, and results". Stefan R. Martin, Robert O. Gappinger, Frank M. Loya, Bertrand P. Mennesson, Samuel L. Crawford, Eugene Serabyn. Proc. SPIE Vol. 5170, p. 144-154, Techniques and Instrumentation for Detection of Exoplanets; Daniel R. Coulter; Ed. Nov 2003.
5. "Mid-IR interferometric nulling for TPF", Wallace, James K.; Babiwale, Vivek; Bartos, Randy; Brown, Ken; Gappinger, Robert; Loya, Frank; MacDonald, Dan; Martin, Stefan; Negron, John; Truong, Tuan; Vasisht, Gautam. Proceedings of SPIE Volume: 5491. "New Frontiers in Stellar Interferometry". Editor(s): Traub, Wesley A. Published: 10/2004
6. "The Keck interferometer nuller: system architecture and laboratory performance". Serabyn, Eugene; Booth, Andrew J.; Colavita, M. M.; Creech-Eakman, Michelle J.; Crawford, Samuel L.; Garcia, Jean; Johnson, Richard L., Jr.; Hovland, Erik; Koresko, C.; Ligon, Edgar R.; Martin, Stefan R.; Mennesson, Bertrand P.; Moore, James D.; Palmer, Dean L.; Paine, Christopher G.; Shao, Michael; Swain, Mark R.; Smythe, Robert F.; Vasisht, Gautam. Proceedings of SPIE Volume: 5491. "New Frontiers in Stellar Interferometry". Editor(s): Traub, Wesley A. Published: 10/2004
7. "Keck Interferometer status and plans". Colavita, M. M.; Wizinowich, Peter L.; Akeson, Rachel L. Proceedings of SPIE Volume: 5491. "New Frontiers in Stellar Interferometry". Editor(s): Traub, Wesley A. Published: 10/2004
8. "Deep nulling of laser light in a rotational shearing interferometer", Stefan R. Martin, Eugene Serabyn, Graham Hardy. Proc. SPIE Vol. 4838, p. 656-667, Interferometry for Optical Astronomy II; Wesley A. Traub; Ed. Feb 2003.
9. "Dynamic Simulations for the Terrestrial Planet Finder Interferometer", Ying-Yong Li. At this meeting.